**SLAC TRANS – 0227**

# TRANSLATION

**TITLE** : — as translated into ENGLISH FROM RUSSIAN

ESTIMATES OF ELECTROMAGNETIC BACKGROUND PROCESSES FOR THE VLEPP PROJECT

**AUTHOR(S)** : M. S. Zolotarev et al.

**SOURCE** : Inst. Yadernoi Fiziki, Preprint 81–63

**TRANSLATED** : June 1987

**FOR** : Stanford Linear Accelerator Center
Stanford, California

**BY** : AD–EX Translations International/USA

# ESTIMATES OF ELECTROMAGNETIC BACKGROUND PROCESSES FOR THE VLEPP PROJECT

M. S. Zolotarev, E. A. Kuraev, and V. G. Serbo[1]

Inst. Yadernoi Fiziki (Siberian Branch, USSR Acad. Sci)

Preprint 81-63

## Abstract

We discuss the electromagnetic background processes for the VLEPP project, a linear colliding electron-positron beam project with energy 2E = 200-600 GeV currently under development at the Institute for Nuclear Physics (Siberian Branch, USSR Academy of Sciences). In this project, we propose to obtain high accelerator luminosity with relatively rare collisions between dense $e^+e^-$ clumps. These clumps contain large electric and magnetic (~1 MGauss) fields. The particles in the colliding beam emit hard photons (with energies ~1 GeV) as they move in these fields. The number of background events arising both in interactions between these photons and electrons and photons from the colliding beam in ordinary $e^+e^-$ collisions (brehmsstrahlung, creation of $e^+e^-$ pairs, etc.) are estimated.

---

[1]Novosibirsk State University

Contents

## 1. Introduction

In the plan for an electron-positron beam collider (VLEPP, [1]) with an energy of $\sqrt{s} = 2E = 200\text{-}600$ GeV, we propose to have two $e^+$ and $e^-$ clumps colliding at a frequency ~10 Hz, with $N \sim 10^{12}$ in each clump. With a projected luminosity of $10^{32}$ $cm^2 sec^{-1}$, the integrated luminosity per collision,

$$L = 10^{31}\ cm^{-2} = 10^{-2}\ \text{nanobarn}^{-1}. \qquad (1)$$

Since $L \sim N^2/S_e$, the cross section of the clump $S_e \sim 10^{-7}$ $cm^2$. The electric E and magnetic B field for a cylindrical clump so small in area at the relatively high current of $J \sim eNc/\ell \sim 5$ kA ($\ell \sim 1$ cm is the length of the clump) are very large: $E \sim B \sim 10$ MGauss. In this case, the energy losses due to emission from the particles in the E and B fields of the colliding clumps, $\Delta E$, turn out to be large: $\Delta E \sim E$. In order to reduce these losses and preserve monochromaticity of the beams to a level of 1%, we propose to use lenticular clumps (elliptical in cross section in the xy plane, with semiaxes a and b, with $b \ll a$, conserving the area $S_e = \pi ab$) to reduce the field. Since great technical difficulties are involved in

obtaining small values of $b/a$, the choice of $b/a$ is determined by the requirement

$$\eta \equiv \Delta E/E = 10^{-2}. \qquad (2)$$

Under these conditions, the fields are reduced to a magnitude of order $E \sim B \sim 1$ MGauss. However, each $e^{\pm}$ emits several photons with energy ~1 GeV as it moves in fields of this size. These photons fly off at small angles $\lesssim 1/\gamma$ to the particle trajectory ($\gamma = E/mc^2 > 10^5$). However, the interaction of these photons with photons or electrons in the opposing clump leads to the appearance of high-energy charged particles and neutral particles moving off at large angles. These are precisely the particles which will evidently be the main background source for future detectors.

The fields within the clump vary along the $y$ axis from $E \sim B \sim 0$ at the center of the clump to $E \sim B \sim$ 1 MGauss at the edge of the clump. When an electron moving along the $z$ axis finds itself in such a field, it executes approximately one oscillation along the $y$ axis. Thus, averaging over $y$ must be carried out both when estimating the radiative loss (2) and when estimating $dn(\omega)$ - the number of photons in the frequency interval from $\omega$ to $\omega + d\omega$. Moreover, these oscillations mean that some of the

photons formed (mainly the soft photons) will fly off at an angle $\sim 2\pi b/\ell \sim 10^{-4}$ and only partially interact with the photons and positrons in the opposing clump. Since the photons themselves are formed in the process of the collision between the $e^+e^-$ clumps, each photon in one clump is able to react with roughly speaking only half of the electrons or 1/4 of the photons in the opposing clump.[2] Suppose we are interested in some finite state f; the number of photon events for $\gamma e^{\pm}$ for <u>one</u> collision between the $e^+e^-$ clumps is then

$$N_{\gamma e^{\pm}\to f} \sim \tfrac{1}{2} L \int dn(\omega)\, d\sigma_{\gamma e^{\pm}\to f}(\omega). \tag{3}$$

Analogously, for $\gamma\gamma$ collisions

$$N_{\gamma\gamma\to f} \sim \tfrac{1}{4} L \int dn(\omega_1)\, dn(\omega_2)\, d\sigma_{\gamma\gamma\to f}(\omega_1, \omega_2). \tag{4}$$

<u>Estimates of the E and B fields</u>

The fields within a clump are determined by the charge density $\rho$; it is suggested in [2] that $\rho = (2eN/\pi ab\ell)\sin^2(\pi z/\ell)$ for $0 \le z \le \ell$, $(x/a)^2 + (y/b)^2 \le 1$. From this, we may estimate the fields within the clump:

---

[2]For example, these relationships may be derived under the assumption of constant beam density (see Appendix I).

$$\mathcal{E} \sim B \sim \pi^2 \rho y = B_0 \frac{y}{\beta} \sin^2 \frac{\pi z}{\ell}, \qquad B_0 = \frac{2\pi e N}{a\ell}. \tag{5}$$

The accelerations due to the electric and magnetic fields for an electron moving parallel to the z axis (at a given distance y from it) are identical in magnitude and direction. Taking this into account, the energy losses $\Delta E$ due to radiation over the flight time $T_0 = \ell/2C$ are (see [3], § 74)

$$\Delta E \sim \frac{8}{3} r_e^2 c \gamma^2 \int_0^{T_0} B^2 dt = \frac{4}{3} r_e^2 \gamma^2 \int_0^{\ell} B^2 dz =$$

$$= \frac{\ell}{2} \left( \frac{\gamma r_e y B_0}{\beta} \right)^2, \qquad r_e = \frac{e^2}{mc^2}.$$

After averaging over y, we have (taking the value of $B_0$ from (5) into account)

$$\eta = \frac{\Delta E}{E} = \frac{2\pi^2}{3} \frac{r_e^3}{a^2 \ell} N^2 \gamma. \tag{6}$$

whence we find

$$a = \pi r_e N \left( \frac{2\gamma r_e}{3\eta \ell} \right)^{1/2}, \quad \beta = \frac{S_e}{\pi a}, \quad B_0 = \frac{2e}{r_e \ell} \left( \frac{3\eta \ell}{2\gamma r_e} \right)^{1/2}. \tag{7}$$

The clump parameters thus obtained (taking into account (2)) are given in Table 1.

We shall now estimate the mean number of electron (positron) oscillations in the magnetic field within the colliding clumps. Since the electron velocity is nearly

parallel to the beam axes, the forces acting on the electron due to the electric and magnetic fields are identical in magnitude and direction, so that $F_y = -2eE = -2eB_0 \frac{y}{b} \sin^2 \frac{\pi z}{\rho}$. After averaging over $y$, the equation of motion of the electron in the transverse direction will take the form

$$m\gamma \ddot{y} = \langle F_y \rangle = -\frac{eB_0}{\beta} y,$$

i. e., the oscillations will be harmonic. The period of the transverse oscillations $T$ is given by

$$T = T_0 \left( \frac{8\gamma S_e}{r_e \ell N} \right)^{1/2},$$

where $T_0 = \ell/2c$ is the time of flight for an electron through the colliding clump. Hence, we obtain a value of order unity for the number of transverse electron oscillations:

$$\frac{T}{T_0} = \begin{cases} 0.75 & \text{for } E = 100 \text{ GeV}, \\ 1.3 & \text{for } E = 300 \text{ GeV}. \end{cases}$$

## 3. Photon Spectrum

As is well known (see [3], §74), the number of photons emitted by an electron in a homogeneous magnetic field $H$ during a time $dt$ is equal to

$$d\tilde{n}(\omega) = \frac{\sqrt{3}}{2\pi}\,\frac{\alpha e H}{mc}\,F\!\left(\frac{\omega}{\tilde{\omega}_c}\right)\frac{d\omega}{\omega}\,dt\,, \qquad (8)$$

$$\tilde{\omega}_c = \frac{3}{2}\,\frac{eH}{mc}\,\gamma^2\,.$$

where $F(x)$ is defined in terms of the MacDonald function $K_\nu(x)$ as follows:

$$F(x) = x\int_x^\infty K_{5/3}(\xi)\,d\xi = \begin{cases} 2^{2/3}\,\Gamma(2/3)\,x^{1/3}\,, & x \ll 1 \\ \sqrt{\frac{\pi x}{2}}\,e^{-x}\,, & x \gg 1. \end{cases} \qquad (9)$$

A graph of this function is shown in Fig. 1. We also present the following integral equations which will be useful below:

$$\int_0^\infty F(x)\,dx = \frac{8\sqrt{3}\,\pi}{27}\,, \quad \int_0^\infty F(x)\,\frac{dx}{x} = \frac{5\pi}{3}\,. \qquad (9a)$$

The number of photons $dn(\omega)$ (which is what we are interested in) in fields (5) is determined from $d\tilde{n}(\omega)$. We replace the homogeneous field $H$ by $H_{eff} = 2B_0$ from (5), integrate with respect to time $t = z/2c$ from 0 to $T_0 = \ell/2c$, and average the result over $y$. The result is

$$dn(\omega) = \frac{\sqrt{3}}{2\pi}\,\frac{\alpha e B_0 \ell}{mc^2}\,\frac{d\omega}{\omega}\int_0^\ell \frac{dz}{\ell}\int_0^b \frac{dy}{b}\,\frac{B(y,z)}{B_0}\,F\!\left(\frac{\omega B_0}{\omega_c B(y,z)}\right), \qquad (10a)$$

$$\omega_c = 3\,\frac{eB_0}{mc}\,\gamma^2\,.$$

It is convenient to transform this expression to a form analogous to (8), replacing the function $F(\omega/\tilde{\omega}_c)$ by the new function $\varphi(\omega/\omega_c)$, which is normalized so that

$$\int_0^\infty F(x)\,dx = \int_0^\infty \varphi(x)\,dx. \tag{11}$$

Then[3]

$$dn(\omega) = A\,\varphi\left(\frac{\omega}{\omega_c}\right)\frac{d\omega}{\omega}, \quad A = \frac{\sqrt{3}}{16\pi}\,\frac{\alpha e B_0 l}{mc^2},$$

$$\varphi(x) = \frac{16}{\pi}\,x^{\frac{3}{2}}\int_x^\infty \frac{\sqrt{\xi - x}}{\xi^3}\,F(\xi)\,d\xi. \tag{10b}$$

Using $B_0$ from (7), we find that

$$A = \frac{3\alpha}{8\pi}\left(\frac{\gamma l}{2\gamma r_e}\right)^{1/2}, \quad \omega_c = \frac{6c\gamma^{3/2}}{l}\left(\frac{3\gamma l}{2r_e}\right)^{1/2}.$$

Using property (9), we obtain the asymptotic expressions

$$\varphi(x) = \begin{cases} \varphi_1 x^{1/3} \text{ for } x \ll 1; & \varphi_1 = \dfrac{2^{2/3}\,36}{5\sqrt{3}}\,\Gamma\left(\dfrac{7}{6}\right) \approx 6 \\ \dfrac{4\sqrt{2}}{x}\,e^{-x}, & x \gg 1 \end{cases} \tag{12}$$

and the integral relations

---

[3]It is convenient in (10a) to make the change of variables $\omega B_0/\omega_c B(y, z) = \xi$, $u = \xi y/b$ and integrate with respect to u.

$$\int_0^\infty \varphi(x)\,dx = \frac{8\sqrt{3}\,\pi}{27}\,, \quad \int_0^\infty \varphi(x)\,\frac{dx}{x} = \frac{10\pi}{3}\,. \qquad (13)$$

A graph of $\varphi(x)$ is shown in Fig. 1. It is important to note that the so-called critical frequency $\omega_c$ (which specifies the frequency scale above which the spectrum falls off exponentially) is determined by the maximum value of the field $B_0$ rather than the mean value. However, just as might be expected, the maximum in $\varphi(x)$ is shifted to smaller values of $x$.

Using (13), we then obtain the mean number of photons $n$ and the mean photon frequency $\langle \omega \rangle$ (see Table I):

$$n = \int dn(\omega) = \frac{40\pi}{3} A = \frac{5\alpha}{4}\left(\frac{\eta l}{2\gamma r_e}\right)^{1/2},$$

$$\langle\omega\rangle = \frac{1}{n}\int \omega\, dn(\omega) = \frac{4\sqrt{3}}{45}\,\omega_c \approx 0{,}154\,\omega_c\,.$$

Fig. 1

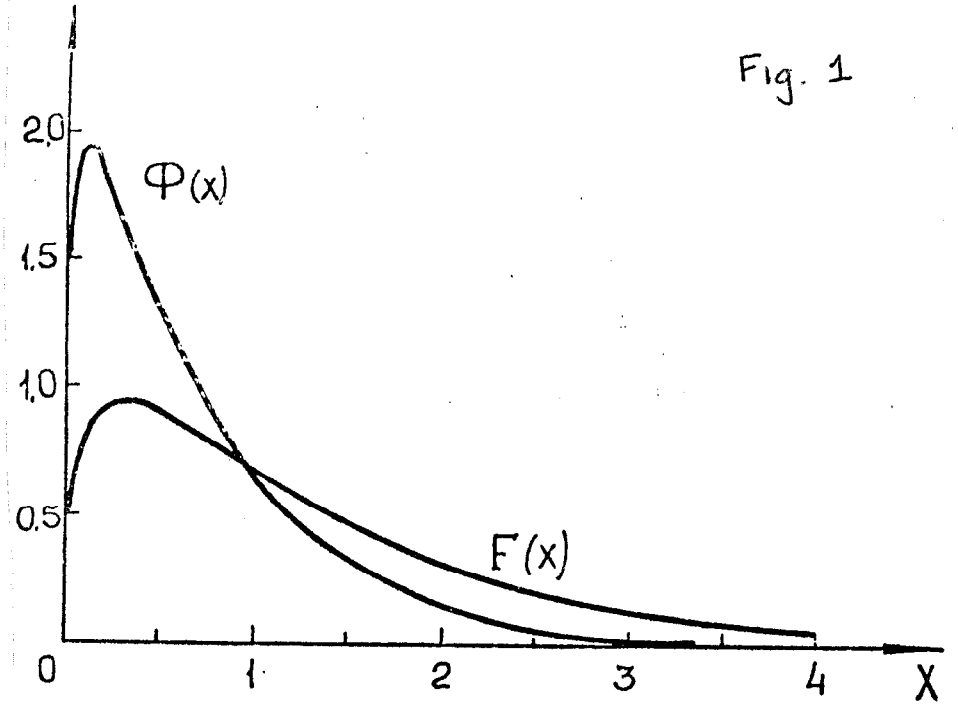

Table I

| $N = 10^{12}$, $L = 10^{31}$ cm$^{-2}$, $\eta = \Delta E/E = 10^{-2}$, $\ell$ = 1 cm | | | |
|---|---|---|---|
| $E = \sqrt{s}/2$, GeV | | 100 | 300 |
| Transverse dimensions of beam | 2a, $\mu$m | 34 | 59 |
| | 2b, $\mu$m | 0.37 | 0.22 |
| $E_{max} + B_{max} = 2B_0$, MGauss | | 3.5 | 2.0 |
| Critical frequency, $\hbar\omega_c$, GeV | | 2.4 | 12 |
| Mean photon energy, $\langle \hbar\omega_c \rangle$, GeV | | 0.36 | 1.9 |
| Number of photons, n | | 2.8 | 1.6 |
| Constant A in spectrum (10) | | 0.26 | 0.15 |

## 4. Recording Conditions. Main Notation

Processes with multiparticle final states should make up a large fraction of the physically interesting processes. It is desirable to have a detector with solid angle close to $4\pi$ to record them. However, the number of background particles

moving at small angles in one $e^+e^-$ collision is very large. It will apparently be exceptionally difficult to carry out measurements at small angles under these conditions.

Below, we shall estimate the number of background events per collision between $e^+e^-$ clumps when the final particles $f$ are moving in the interval of angles $\theta_0 \leq \theta_f \leq \pi - \theta_0$ (the angle $\theta$ is, for definiteness, measured from the direction of the $e^-$ beam) and a final energy $\epsilon_f$ larger than some threshold energy $\epsilon_0$. It was assumed for purposes of estimation that $\epsilon_0$ is much larger than the mass of the final particle and that the angle $\theta_0 \sim 10^\circ$-$60^\circ$.

Thus, for a particle with energy $\epsilon_f$ and an angle of escape $\theta_f$, we have

$$\epsilon_f \geq \epsilon_0 , \quad -c_0 \leq c = \cos\theta_f \leq c_0 , \quad c_0 = \cos\theta_0 . \qquad (15)$$

Throughout the remainder of the paper, we shall use a system of units where

$$\hbar = c = 1$$

Note the useful relation

$$\frac{\alpha^2}{1\,GeV^2} L = 0{,}21,$$

where the luminosity $L = 10^{-31}$ cm$^{-2}$. In addition to the

notation just indicated, we shall also use the following:

$s_0 = \sin \theta_0$

$\omega_c$ is the critical frequency (see (10a) and Table I),

$$x_0 = \frac{\varepsilon_0}{2\omega_c}(1-c_0) \quad , \qquad y_0 = \frac{\varepsilon_0}{2\omega_c}(1+c_0) \, ,$$

$$x_c = \frac{\varepsilon_0}{2\omega_c}(1-c) \quad , \qquad y_c = \frac{\varepsilon_0}{2\omega_c}(1+c) \, ,$$

$$2 = \frac{\varepsilon_0}{\omega_c} = x_0 + y_0 = x_c + y_c \, .$$

5. Compton Scattering

a) We shall discuss the scattering of $e^-$ on photons from the oncoming clump. The energy of an electron scattered by an angle of $\theta_e$ ($c = \cos \theta_e$) is

$$\varepsilon_f \equiv E' = \frac{2E\omega}{E(1-c)+\omega(1+c)} \, . \tag{18}$$

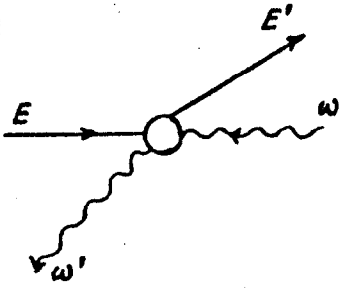


Fig. 2

The number of background $e^-$ is, according to (3), equal to

where $d\sigma(\omega, c)$ is the cross section for the Compton effect, and the limits of integration are determined by conditions (15). We shall see below that the main contribution to the integral is provided by the frequency region $\omega \sim \epsilon_0 (1 - c)$. Under the condition $\epsilon_0 \ll E$, we have $\omega \ll E(1 - c)$, the expressions for $E'$ (18) and $d\sigma(\omega, c)$ become simpler:

$$E' = \frac{2\omega}{1-c}, \qquad d\sigma(\omega,c) = \frac{\pi\alpha^2}{E\omega} \cdot \frac{dc}{1-c^2} \tag{19}$$

and we find that

$$N_{e^-\gamma\to e^-} = \frac{\pi\alpha^2 LA}{2E\omega_c} J_e, \quad J_e = \int_{-c_0}^{c_0} \frac{dc}{1-c^2} \int_{x_c}^{\infty} \Phi(x) \frac{dx}{x^2}. \tag{20}$$

The integral $J_e$ is evaluated for large and small values of the parameter $x_0$ in Appendix 2; the answer takes the form

$$N_{e^-\gamma\to e^-} = \frac{\alpha^2 LA}{E} \begin{cases} \dfrac{22{,}4}{\xi_0^{2/3}\omega_c^{1/3}} f_1(\theta_0), & x_0 \ll 1 \\ \dfrac{8{,}9}{\omega_c x_0^4 (1+c_0)} e^{-x_0}, & x_0 \gg 1, \end{cases} \tag{21}$$

where the exact form of $f_1(\theta_0)$ is given in (A4); the following asymptotic expressions are convenient for estimates:

$$f_1(\theta_0) = \int_{-c_0}^{c_0} \frac{dc}{(1+c)(1-c)^{5/3}} = \begin{cases} \dfrac{1{,}19}{\theta_0^{4/3}} + 0{,}63 \ln\dfrac{1}{\theta_0} + 0{,}77, & \theta_0 \ll 1 \\ 2c_0\left(1 + \dfrac{14}{27} c_0^2\right), & c_0 \ll 1. \end{cases}$$

b) We shall now discuss the exact same process under conditions where the particle being recorded is a photon. Repeating the calculational procedure from the preceding case, we obtain ($c = \cos\theta_\gamma$)

$$\varepsilon_f \equiv \omega' = \frac{2E\omega}{E(1-c)+\omega(1+c)}, \quad d\sigma = \frac{2\pi\alpha^2}{E^2}\cdot\frac{dc}{(1-c)^2} f\left(\frac{\omega}{\omega_E}\right), \tag{22a}$$

$$f(t) = \frac{1+(1+t)^2}{2(1+t)^3}, \quad \omega_E = \frac{E(1-c)}{1+c};$$

$$N_{e^-\gamma\to\gamma} = \frac{\pi\alpha^2 LA}{E^2} J_\gamma, \quad J_\gamma = \int_{-c_0}^{c_0}\frac{dc}{(1-c)^2}\int_{x_c}^{\infty}\varphi(x) f\left(x\frac{\omega_c}{\omega_E}\right)\frac{dx}{x}. \tag{22b}$$

We now turn our attention to the fact that the function $f \simeq 1$ outside of the small-angle region (for $\omega \ll \omega_E$), while $f \ll 1$ for small angles (for $\omega \gg \omega_E$). Because of the good convergence of the integral over $x$ in (22b), we may set $f = 1$ in our parametr range. After calculating $J_\gamma$ (see Appendix 3)

$$N_{e^-\gamma\to\gamma} = \frac{\alpha^2 LA}{E^2(1-c_0)} \begin{cases} 65{,}8\,\dfrac{c_0}{1+c_0}, & x_0 \ll 1 \\ \dfrac{17{,}8}{x_0^3}\,e^{-x_0}, & x_0 \gg 1. \end{cases} \tag{23}$$

Note that the number of background events is a very weak function of the recording threshold $\varepsilon_0$ for $x_0 \ll 1$: $N_{e\gamma\to e} \sim \varepsilon_0^{-2/3}$, and $N_{e\gamma\to e}$ is independent of $\varepsilon_0$. This difference is due to the fact that in the first case the initial electron "selects" an appropriate partner from the photon spectrum (the main region has $\theta \sim \theta_0$ and $\omega \sim \varepsilon_0(1 - c_0)$ ), and the energy of the scattered electron $E' \sim \varepsilon_0$. In the second case, the main region has $\theta \sim \theta_0$ and $\omega \sim$

$\omega_c$, so that the photon is scattered backwards, and has energy $\omega' \sim \omega_c/(1-c_0) \gg \epsilon_0$.

## 6. $e^+e^- \to e^-e^+\gamma$ Brehmsstrahlung

a) For the basic results on the angular distribution and energy distribution for this process, see (for example) the review paper by Baier, Kuraev, Fadin, and Khoze [4].

We shall first discuss the case where $e^-$ particles are being recorded. The main contribution in this case comes from the Feynman diagram in Fig. 3a, where the upper line corresponds to Compton scattering of an equivalent photon emitted by a positron on an electron (cf. Fig. 2). The equivalent photon spectrum is given by the following formula:

$$dn_\gamma(\omega) = \frac{\alpha}{\pi} l \frac{d\omega}{\omega}, \quad l = \ln \frac{\varepsilon_i^2(1-c^2)}{(m\omega/E)^2}. \tag{24}$$

Fig. 3

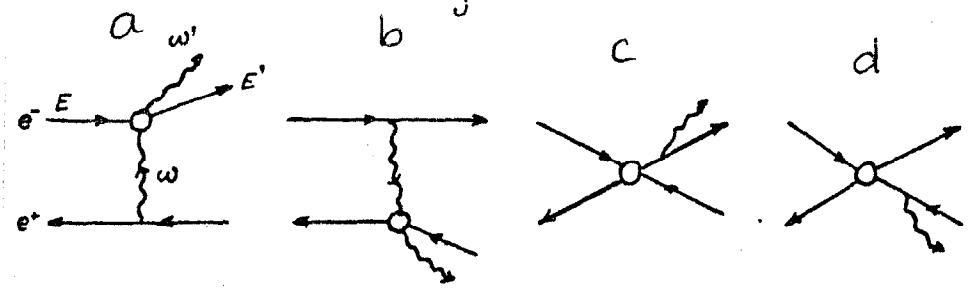


The rest of the discussion is completely analogous to that

carried out in Section 5a for a collision between an $e^-$ and a real photon. The result is

$$N_{e^-e^+\to e^-} = \frac{\alpha^3 L}{E}\int_{-c_0}^{c_0}\frac{dc}{1-c^2}\int_{\varepsilon_0(1-c)/2}^{\infty}\ell\,\frac{d\omega}{\omega^2} = \tag{25}$$

$$= \frac{\alpha^3 L}{E\,\varepsilon_0}\left(\frac{c_0}{1-c_0^2}+\frac{1}{2}\ln\frac{1+c_0}{1-c_0}\right)\ell n\,\frac{E^2(1+c_0)}{m^2(1-c_0)}\ .$$

b) We now discuss the case where the particles recorded are photons. In this case, the main contribution comes from the four Feynman diagrams in Figs. 3a-d. The first two may be discussed in the equivalent photon approximation. In particular, the discussion for the Feynman diagram in Fig. 3a is completely analogous to that for the Compton effect when a photon is recorded (see Section 5b), with dn being replaced by $dn_\nu$ (24). In sum, the contribution from this Feynman diagram is

$$N_{e^-e^+\to\gamma} = \frac{2\alpha^3 L}{E^2}\int_{-c_0}^{c_0}\frac{dc}{(1-c)^2}\int_{\varepsilon_0(1-c)/2}^{E}\frac{d\omega}{\omega}\,f\left(\frac{\omega}{\omega_E}\right)\ell n\,\frac{E^2\omega'^2(1-c^2)}{(m\,\omega)^2}\ .$$

The logarithmic integral over $\omega$ is cut off at $\omega \sim \omega_E$, since the function $f(\omega/\omega_E) \sim 1/\omega$ for $\omega > \omega_E$; therefore, to logarithmic accuracy

$$N^a_{e^-e^+\to\gamma} = \frac{4\alpha^3 L}{E^2}\,\frac{c_0}{1-c_0^2}\,\ell n\,\frac{E}{\varepsilon_0}\,\ell n\,\frac{E^2(1+c_0)}{m^2(1-c_0)}\ .$$

Feynman diagram 3b yields exactly the same contribution. We

emphasize that this contribution is proportional to $1/E^2$. The Feynman diagrams in Figs. 3c and 3d, where the diagram shows the process of large-angle $e^+e^-$ scattering with the subsequent emission of a brehmsstrahlung photon parallel to the $e^+$ and $e^-$ is of the same order. The cross section corresponding to the diagram in Fig. 3c is of the form (see (3.20) in [4]):

$$d\sigma_{3c} = \frac{\alpha^3}{8E^2}\,\frac{d\omega'}{\omega'}\left(1-\frac{\omega'}{E}+\frac{\omega'^2}{2E^2}\right)\cdot\left(\frac{3+c^2}{1-c}\right)^2\cdot \ln\frac{E^2(1-c^2)}{m^2}\cdot dc\ .$$

Hence, we have the following expression for the number of background events:

$$N^b_{e^-e^+\to\gamma} = \frac{\alpha^3}{8E^2}\ln\frac{E}{\varepsilon_0}\ln\frac{E^2(1-c_0^2)}{m^2}\int_{-c_0}^{c_0}\left(\frac{3+c^2}{1-c}\right)^2 dc$$

The diagram in Fig. 3d yields eaxctly the same contribution. Interference between the diagrams in Figs. 3a-3d is negligibly small, since the kinematic regions over which they are important are different; thus, the total number of photon events is

$$N_{e^-e^+\to\gamma} = 2\left(N^a_{e^-e^+\to\gamma} + N^b_{e^-e^+\to\gamma}\right)\ . \qquad (26a)$$

For small angles ($\theta \ll 1$)

$$N_{e^-e^+\to\gamma} = \frac{16\alpha^3 L}{(E\theta_0)^2}\ln\frac{E}{\varepsilon_0}\ln\frac{E^2}{m^2} \qquad (26b)$$

## 7. Processes involving the formation of $e^-e^+$ (or $\mu^-\mu^+$) pairs

We shall now discuss the following three processes

$\gamma\gamma \to e^-e^+$ (Fig. 4),

$e^- \to e^-e^-e^+$ (Bethe-Heitler process, Fig. 5) (27)

$e^-e^+ \to e^-e^+e^-e^+$ (Landau-Lifshitz process, Fig. 6),

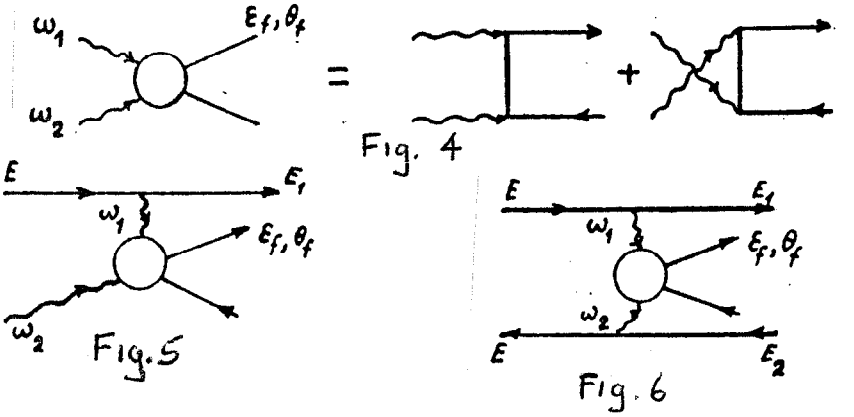


Fig. 4

Fig. 5

Fig. 6

in which $e^-e^+$ pairs (or $\mu^-\mu^+$ pairs) are formed in collisions between real or virtual photons. The number of real photons is given by the spectrum $dn(\omega)$ (10), and the number of virtual (or equivalent) photons is given by the spectrum $dn_v(\omega)$ (24). Since the initial $e^{\mp}$ are scattered at extremely small angles $\lesssim \sqrt{m/E}$, the number of events in which the $e^{\pm}$ are scattered by a noticeable angle $\gtrsim 10^{\circ}$ will be determined only by the $e^{\pm}$-created pairs.

In a collision between photons having energies $\omega_1$ and $\omega_2$, an electron created at an angle $\theta_f$ has energy (cf.(18))

$$\varepsilon_f = \frac{2\omega_1\omega_2}{\omega_1(1-c)+\omega_2(1+c)}\,, \qquad c = \cos\theta_f\,, \tag{28}$$

and the cross section for this process is

$$d\sigma = \frac{\pi\alpha^2}{\omega_1\omega_2}\cdot\frac{dc}{1-c^2}\cdot f\,; \quad f = \frac{\omega_1^2(1-c)^2+\omega_2^2(1+c)^2}{[\omega_1(1-c)+\omega_2(1+c)]^2}\,. \tag{29a}$$

Since $\frac{1}{2} < f < 1$, we shall assume

$$f = 1 \tag{29b}$$

for the estimates below. The limits of integration over photon energy are determined by conditions (15). The limits are shown for a fixed value of $c$ in Fig. 7 (cross-hatched area), where the boundary energies $\omega_\pm$ and the boundary curve $\omega_b$ are

$$\omega_\pm = \tfrac{1}{2}\,\varepsilon_0(1\pm c)\,, \quad \omega_b = \frac{\omega_2\omega_+}{\omega_2-\omega_-}\,. \tag{30}$$

As a result,

$$N_{ab\to e^-} = g\,\pi\alpha^2 L\cdot\int_{-c_0}^{c_0}\frac{dc}{1-c^2}\int_{\omega_-}^{\infty}\frac{dn_2(\omega_2)}{\omega_2}\int_{\omega_b}^{\infty}\frac{dn_1(\omega_1)}{\omega_1}\,,$$

where, in agreement with (3)-(4), $g = \frac{1}{4}$, $\frac{1}{2}$, or $1$ for $ab = \gamma\gamma$, $e^-\gamma$, or $e^-e^+$.

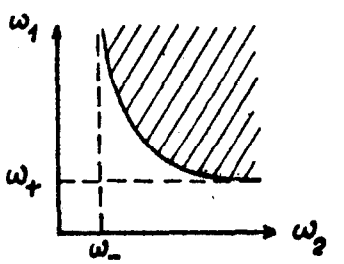


Fig. 7

a) The Landau-Lifshitz process. We use equation (24) for $dn_{1,2}$; the approximate answer is of the form

$$N_{e^-e^+\to e^-} = \frac{2\alpha^4 L}{\pi\,\varepsilon_0^2}\left[\frac{c_0}{1-c_0^2} + \frac{1}{2}\ln\frac{1+c_0}{1-c_0}\right]\cdot\left(\ln\frac{E^2}{m^2}\right)^2. \qquad (31)$$

b) The Bethe-Heitler process. Substituting in $dn_1$ (24) and $dn_2$ (10), integrating over $\omega_1$, and making the substitution $x = \omega_2/\omega_c$, we obtain

$$N_{e^-\gamma\to e^-} = \frac{\alpha^3 LA}{\varepsilon_0\,\omega_c}\,J_{e\gamma}\,; \qquad J_{e\gamma} = \int_{-c_0}^{c_0}\frac{dc}{(1-c)(1+c)^2}\int_{x_c}^{\infty}\frac{dx}{x^2}\left(1-\frac{x_c}{x}\right)\Phi(x). \qquad (32)$$

The calculation of $\Phi_{e\gamma}$ is carried out in Appendix 4; the answer is of the form

$$N_{e^-\gamma\to e^-} = \alpha^3 LA\cdot\begin{cases} \dfrac{8{,}6\,f_2(\theta_0)}{\varepsilon_0^{5/3}\,\omega_c^{1/3}}\ln\dfrac{E^2(1+c_0)}{m^2(1-c_0)}, & \dfrac{\varepsilon_0}{\omega_c}\ll 1 \\ \dfrac{5{,}1}{\varepsilon_0^{5/3}\,\omega_c^{1/3}\,\theta_0^{4/3}}\ln\dfrac{E^2\theta_0^2}{m^2}, & \dfrac{\varepsilon_0}{\omega_c}\gg 1,\ \dfrac{\varepsilon_0\theta_0^2}{\omega_c}\ll 1 \\ \dfrac{5{,}7\,e^{-x_0}}{\varepsilon_0\,\omega_c\,x_0^5(1+c_0)^2}\ln\dfrac{E^2(1-c_0)}{m^2(1+c_0)}, & x_0\gg 1 \end{cases} \qquad (33)$$

where the exact form of $f_2(\theta_0)$ is given in (A8); the following asymptotic expressions are convenient for claculation:

$$f_2(\theta_0) = \begin{cases} \frac{0,63}{\theta_0^2} + \frac{0,6}{\theta_0^{4/3}} + 0,53 \ln\frac{1}{\theta_0} + 0,8, & \theta_0 \ll 1 \\ 2c_0\left(1 + \frac{17}{27}c_0^2\right), & c_0 \ll 1 . \end{cases}$$

Note one interesting characteristic of this process at small values of $\theta_0$. At low recording thresholds $\epsilon_0 \ll \omega_c$, the main contribution comes from photons with low energies $\omega_{1,2} \sim \epsilon_0 (1 \pm c)$. In this region, the equivalent photon spectrum ($dn_v \sim \omega_1^{-1}$) is more singular than the real photon spectrum ($dn/d\omega_2 \sim \omega_2^{-1/3}$). Thus, it is advantageous for an equivalent photon to have a smaller energy, so that $\omega_1/\omega_2 \sim (1 + c)/(1 - c) \ll 1$. From this it is evident that the newly created pair moves antiparallel to the initial electron momentum, $\theta \sim \pi \sim \theta_0$. The situation changes somewhat for high thresholds $\epsilon_0 \gg \omega_e$. Since the real photon spectrum falls off exponentially at high energies, it is advantageous for the real photon to have a lower energy. Thus, the newly formed pair moves parallel to the initial electron, $\theta \sim \theta_0$.

c) The process $\gamma\gamma \to e^-e^+$. Using equation (10) for $dn_{1,2}$, we find that

$$N_{\gamma\gamma\to e^-} = \frac{\pi\alpha^2 L A^2}{4\omega_c^2} J_{\gamma\gamma}; \quad J_{\gamma\gamma} = \int_{-c_0}^{c_0} \frac{dc}{1-c^2} \int_{x_c}^{\infty} \frac{dx}{x^2} \Phi(x) \int_{xy_c/(x-x_c)}^{\infty} \frac{dy}{y^2} \Phi(y). \quad (34)$$

After calculating the integral $\mathcal{J}_{\gamma\gamma}$ (see Appendix 5), we find that

$$N_{\gamma\gamma\to e^-} = \alpha^2 L A^2 \begin{cases} \dfrac{10\,y}{\varepsilon_0^{4/3}\omega_c^{2/3}} f_3(\theta_0), & z = \dfrac{\varepsilon_0}{\omega_c} \ll 1 \\ \dfrac{186}{(\varepsilon_0\theta_0)^2 z^2} e^{-z}, & z \gg 1,\ x_0 \cdot y_0 = \left(\dfrac{\varepsilon_0\theta_0}{2\omega_c}\right)^2 \ll 1 \\ \dfrac{504}{\varepsilon_0^2 z^{9/2} s_0^{7/2}(1+s_0)^3 c_0} e^{-2(1+s_0)}, & z \gg 1,\ x_0 \gg 1, \end{cases} \qquad (35)$$

where

$$f_3(\theta_0) = \int_{-c_0}^{c_0} \frac{dc}{(1-c^2)^{5/3}} = \begin{cases} \dfrac{1,5}{\theta_0^{4/3}} + 1,34, & \theta_0 \ll 1 \\ 2c_0\left(1 + \dfrac{5}{9}c_0^2 + \dfrac{4}{9}c_0^4\right), & c_0 \ll 1. \end{cases}$$

Unlike the previous process, the number of particles in this process falls off exponentially $N_{\gamma\gamma\to e^-} \sim \exp(-\epsilon_0/\omega_c)$ for high thresholds $\epsilon_0 \gg \omega_c$, even for small values of $x_0$.

8. Other background processes

We shall now discuss processes in which a $e^+e^-\gamma$ (or $\mu^+\mu^-\gamma$) system is formed in a $\gamma\gamma$, $\gamma e$, or $e^+e^-$ collision (Fig. 8-10) and a photon is observed.

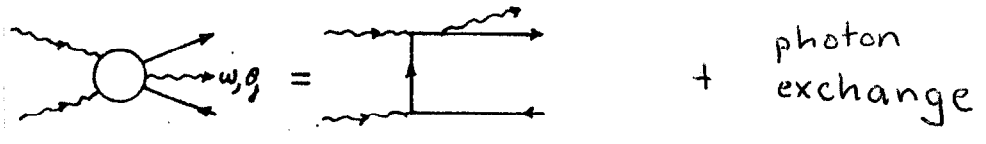


Fig 8.

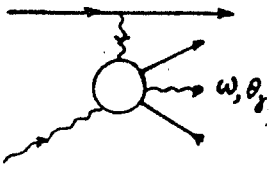


Fig. 9.

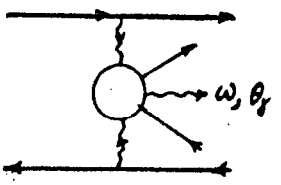


Fig 10.

The number of background events for these processes differs from the number of background processes without emission of a photon (see Figs. 4-6 and equations (35), (33), and (31), respectively) by an additional factor of order

$$\sim \frac{\alpha}{\pi} \ln \frac{\varepsilon_0^2(1-c_0^2)}{m^2} . \qquad (36)$$

As an example, we shall carry out the calculation for the process in Fig. 10. The differential momentum cross section for this process is of the form [5] ($c = \cos\theta_\gamma$, $\varepsilon_f = \omega$)

$$d\sigma_{10} = \frac{14\alpha^5}{3\pi^2} \frac{d\omega}{\omega^3} \frac{dc}{(1-c^2)^2} \left(\ln \frac{E^2}{m^2}\right)^2 \ln \frac{\omega^2(1-c^2)}{m^2} .$$

The limits of integration are determined by conditions (15). The result is

$$N^{10}_{e^+e^-\to\gamma} = \frac{7\alpha^5 L}{3\pi^2 \varepsilon_0^2} \left[\frac{c_0}{1-c_0^2} + \frac{1}{2} \ln \frac{1+c_0}{1-c_0}\right] \left(\ln \frac{E^2}{m^2}\right)^2 \ln \frac{\varepsilon_0^2(1-c_0^2)}{m^2} . \qquad (37)$$

b) For reference, we shall write down the number of background events for two-particle processes

$$N_{e^+e^-\to e^+e^-} = \frac{\pi\alpha^2 L}{16E^2} \int_{-c_0}^{c_0} \left(\frac{3+c^2}{1-c}\right)^2 dc \xrightarrow[\theta_0 \ll 1]{} \frac{2\pi\alpha^2 L}{(E\theta_0)^2} , \qquad (38)$$

$$N_{e^+e^-\to\gamma\gamma} = \frac{\pi\alpha^2 L}{4E^2} \int_{-c_0}^{c_0} \frac{1+c^2}{1-c^2} dc \xrightarrow[\theta_0 \ll 1]{} \frac{\pi\alpha^2 L}{E^2} \ln \frac{2}{\theta_0} , \qquad (39)$$

$$N_{e^+e^-\to\mu^+\mu^-} = \frac{\pi\alpha^2 L}{4E^2} c_0 \left(1 + \frac{1}{3} c_0^2\right) . \qquad (40)$$

9. Results and discussion

The results of calculating the number of background events using equations (21), (23), (25), (26), (31), (33), (35), and (36) are shown in Figs. 11 and 12.

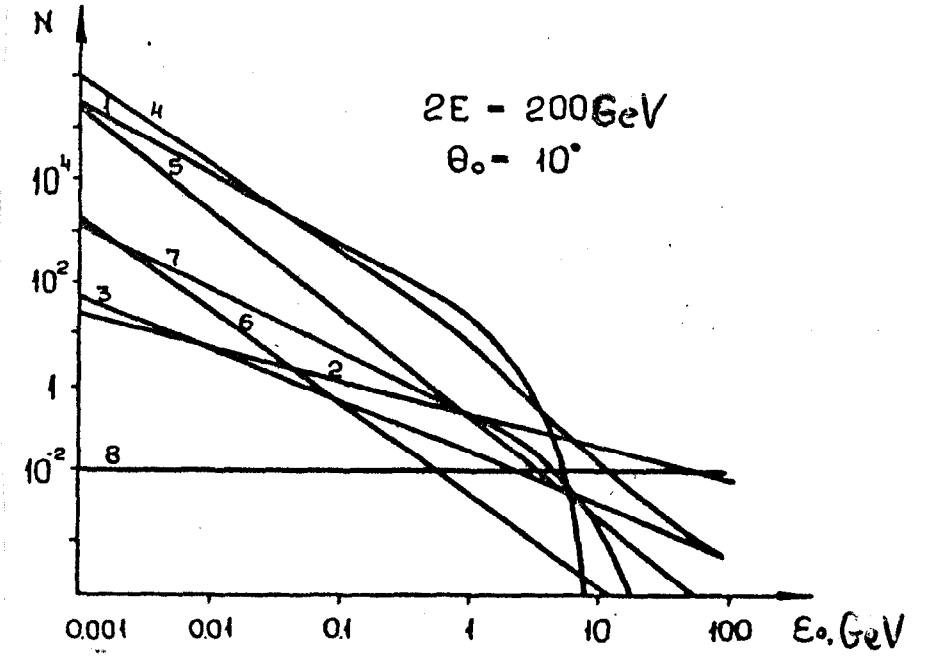


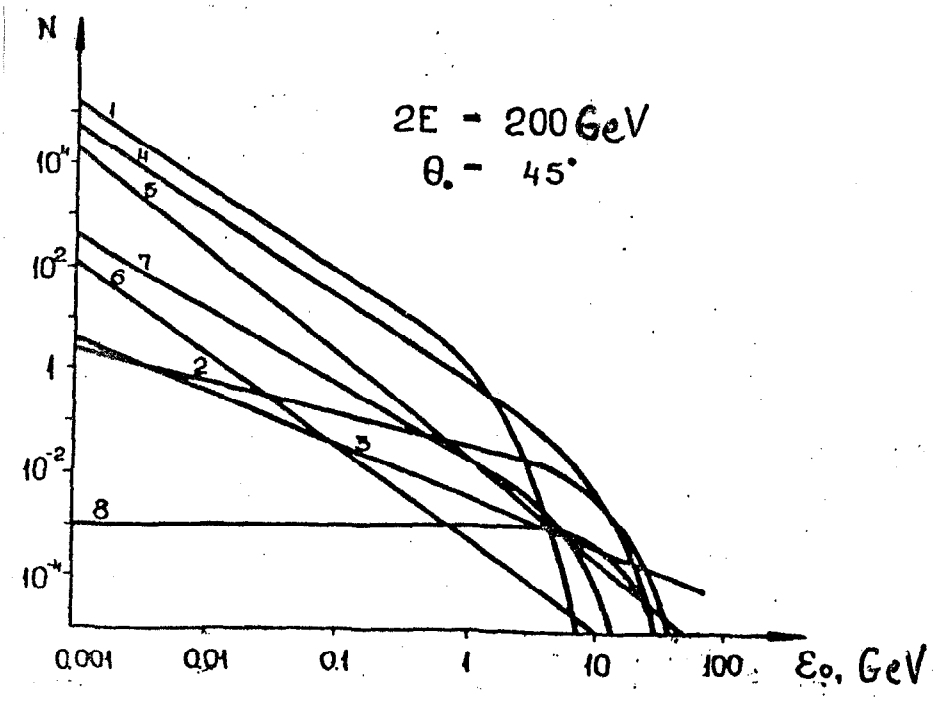

These figures show the number of background events for a single collision between $e^+e^-$ clumps having energies of 100 + 100 GeV. Recall that according to (15), an event is called a background event when the charged particle ($e^\pm$, $\mu^\pm$) or photon has an energy greater than $\epsilon_0$ (the threshold) and moves in the interval of angles $\theta_0 \leq \theta \leq \pi - \theta_0$. The numbers on the curves in figures (1-8) correspond to the following processes:

| | | |
|---|---|---|
| 1. | $\gamma\gamma \to e^+e^-$ $(\mu^+\mu^-)$, | $e^\pm$ or $\mu^\pm$ recorded. |
| 2. | $\gamma e^\pm \to \gamma e^\pm$, | $e^\pm$ recorded. |
| 3. | $e^+e^- \to e^+e^-\gamma$ | $e^\pm$ recorded. |
| 4. | $\gamma e^\pm \to e^\pm e^+e^-$ $(e^\pm\mu^+\mu^-)$ | $e^\pm$ or $\mu^\pm$ recorded. |
| 5. | $e^+e^- \to e^+e^-e^+e^-(e^+e^-\mu^+\mu^-)$ | $e^\pm$ or $\mu^\pm$ recorded. |
| 6. | $e^+e^- \to e^+e^-e^+e^-\gamma$ $(e^+e^-\mu^+\mu^-\gamma)$ | $\gamma$ recorded. |
| 7. | $\gamma e^\pm \to e^\pm e^+e^-$ $(e^\pm\mu^+\mu^-\gamma)$ | $\gamma$ recorded. |
| 8. | $\gamma e^\pm \to \gamma e^\pm$ | $\gamma$ recorded. |

We now note a few characteristic traits of the processes under discussion.

One of the main sources of background at low thresholds is Process 1: $\gamma\gamma \to e^+e^-$. However, its contribution decreases exponentially ($N \sim \exp(-\epsilon_0/\omega_c)$) as the threshold $\epsilon_0$ is increased.

Compton scattering (Curves 2 and 8) yields a relatively small contribution at small thresholds. However, the

contribution from this process becomes decisive as $\epsilon_0$ increases. Major contributions to the number of background events are also made by Processes 4 (Bethe-Heitler) and 5 (Landau-Lifshitz . Their contribution falls off at large $\epsilon_0$, but only as a power law: $N_{\gamma e} \sim 1/\epsilon_0$, $N_{e^+e^-} \sim 1/\epsilon_0^2$.

The backgrounds due to all of the processes increase rapidly as $\theta_0$ decreases. Simple estimation formulae for small angles $\theta_0$ are presented in Appendix 6.

We shall now discuss the number of background events as a function of the energy $E$ of the colliding $e^+e^-$. With the relative radiative losses fixed, the critical frequency $\omega_c$ increases with increasing energy ($\omega_c \sim E^{3/2}$), while the mean number of photons $n$ decreases: $n \sim E^{-1/2}$. This means that $N$ is smaller for low thresholds. However, $N$ is larger for cases where the exponential dependence of $N$ on $\epsilon_0/\omega_c$ is important.

A few concluding notes

The total number of background particles decreases rapidly with increasing energy, so that they will not significantly hinder the study of two-particle or two-jet processes where an energy of order the initial particle energy is released in a narrow cone around each jet. However, the background situation becomes worse when studying multiparticle processes, which may make it difficult to study them.

The VLEPP project is characterized by a low frequency of collision between the $e^{\pm}$ clumps, which results in low power demand on the high-frequency power supply and a high pulsed luminosity. The high pulsed luminosity leads to an increase in the probability for collisions between several pairs of particles in a single passage of the clumps. The number of events in which several high-energy particles formed in various interaction events move away at large angles therefore increases. Under these conditions, it will be difficult to study the elementary $e^+e^-$ interaction event.

In the future, as the energy of the colliding beams is increased, it will evidently be necessary to increase the luminosity; this will lead to a worsening of the experimental background conditions at low collision frequencies.

The authors are indebted to A. N. Skrinskii for defining the problem and to V. E. Balakin, L. M. Barkov, I. F. Ginzburg, G. L. Kotkin, Yu. N. Pestov, V. A. Tayurskii, and V. S. Fadin for useful discussions.

## Appendix I. The number of $\gamma e$ and $\gamma\gamma$ collisions in the uniform-density $e^{\pm}$ clump model.

We shall be discussing the reaction $e^+e^- \to f$. The number of these events per collision between $e^+e^-$ clumps is (see [3], §12)

$$N_{e^+e^-\to f} = 2c\,\sigma_{e^+e^-\to f}\int \rho_+ \rho_- \, dt\, dV\,, \quad dV = S_e\, dz\,, \qquad \text{(A1)}$$

where $\rho_\pm = N_\pm / S_e \ell$ is the number of particles per unit volume of the $e^\pm$ clump, which is assumed to be constant over the volume of the clump. For a given value of t, the integration over z is carried out over the region where the clumps overlap, i. e.,

$$\int dt\, dz = \int_0^{\ell/2c} dt \int_{-ct}^{ct} dz + \int_{\ell/2c}^{\ell/c} dt \int_{-\ell+ct}^{\ell+ct} dz\,. \qquad \text{(A2)}$$

Performing this integral, we find that

$$N_{e^+e^-\to f} = \rho_+ \rho_- S_e \ell^2 \sigma = L\sigma\,, \quad L = \frac{N_+ N_-}{S_e}\,,$$

where L is the luminosity per collision between $e^+e^-$ clumps (1).

The number of photons emitted by a positron (electron) moving parallel to the z axis is proportional to its time of flight through the electron (positron) clump, so that the density of photons created by the positrons (or electrons) at the point z at time t is

$$d\rho_\gamma(\omega) = \rho_\pm \, dn(\omega)\, \frac{ct \pm z}{\ell}\,.$$

Substituting this expression into (A1), we obtain the

following expressions for the number of $\gamma e^- \to f$ and $\gamma\gamma \to f$ per collision between $e^+e^-$ clumps:

$$dN_{\gamma e^- \to f} = 2c\,\sigma_{\gamma e^- \to f}(\omega)\,dn(\omega) \int \rho_+ \rho_- \frac{ct-z}{l}\,dt\,dV = \frac{1}{2} L\,\sigma_{\gamma e^- \to f}(\omega)\,dn(\omega)\,;$$

$$dN_{\gamma\gamma \to f} = 2c\,\sigma_{\gamma\gamma \to f}(\omega_1,\omega_2)\,dn(\omega_1)\,dn(\omega_2) \int \rho_+ \rho_- \frac{ct-z}{l} \cdot \frac{ct+z}{l}\,dt\,dV = \frac{1}{4} L\,\sigma_{\gamma\gamma \to f}(\omega_1,\omega_2)\,dn(\omega_1)\,dn(\omega_2)\,. \quad \text{(A3)}$$

## Appendix II. Calculation of the Compton scattering integral $\varphi_e$ (20)

a) The case $x_0 \ll 1$. The main contribution to the integral comes from the region of small $x \sim x_0$. We can therefore use the asymptotic expression for $\varphi(x)$ at small x (12):

$$J_e = \varphi_1 \int_{-c_0}^{c_0} \frac{dc}{1-c^2} \int_{x_c}^{\infty} \frac{dx}{x^{5/3}} = \frac{3\varphi_1}{2^{1/3}} \left(\frac{\omega_c}{\varepsilon_0}\right)^{2/3} f_1(\theta_0)\,,$$

where

$$f_1(\theta_0) = \int_{-c_0}^{c_0} \frac{dc}{(1+c)(1-c)^{5/3}} = \frac{3}{2^{2/3}\,4} \left[\frac{1}{a^2} - \frac{1}{\beta^2} + \ln\frac{a(1-a)}{\beta(1-\beta)} + \frac{2}{\sqrt{3}} \operatorname{arctg} \frac{\sqrt{3}\,(\beta-a)}{2+\beta+a+2a\beta}\right], \quad \text{(A4)}$$

$$a = \left(\sin\frac{\theta_0}{2}\right)^{2/3}, \qquad \beta = \left(\cos\frac{\theta_0}{2}\right)^{2/3}.$$

b) The case $x_0 \gg 1$. It is convenient to reverse the order of integration and write $\mathcal{J}_e$ as a sum of two terms:

$$\mathcal{J}_e = \mathcal{J}_1 + \mathcal{J}_2 = \left[ \int_{x_0}^{y_0} dx \int_{c_x}^{c_0} dc + \int_{y_0}^{\infty} dx \int_{-c_0}^{c_0} dc \right] \frac{\varphi(x)}{x^2} \cdot \frac{1}{1-c^2} ,$$
$$c_x = 1 - \frac{2\omega_c}{\varepsilon_0} x > -c_0 . \qquad \text{(A5)}$$

Since $x_0, y_0 \gg 1$, we may use the asymptotic expression for $\varphi(x)$ at large $x$ (12), with $\varphi(x) \sim e^{-x}$. It is apparent from this that the main contribution to the integral $\mathcal{J}_1$ (or $\mathcal{J}_2$) comes from the region $x - x_0 \sim 1$ (or $x - y_0 \sim 1$). In the region of angles of interest to us ($\theta_0 < 60^\circ$), the ratio $y_0/x_0 = \cot^2(\theta_0/2) > 3$, i. e., $y_0 - x_0 > 2y_0/3 \gg 1$. Thus, $\mathcal{J}_2/\mathcal{J}_1 \sim \exp[-(y_0 - x_0)] \ll 1$. Moreover, for $x - x_0 \sim 1$, we have

$$c_x = c_0 - \Delta c, \quad \Delta c = \frac{2\omega_c}{\varepsilon_0}(x - x_0) \ll c_0 . \qquad \text{(A6)}$$

Therefore,

$$\mathcal{J}_e \approx \mathcal{J}_1 = 4\sqrt{2} \int_{x_0}^{y_0} \frac{e^{-x}}{x^3} \cdot \frac{\Delta c}{1-c_0^2} dx = \frac{8\sqrt{2}\, e^{-x_0}}{x_0^3 (1-c_0^2)} \left[ 1 + O\left(\frac{1}{x_0}\right) \right] \qquad \text{(A7)}$$

Appendix 3. Calculation of the integral $\mathcal{J}_\gamma$ (22).

a) The case $x_0 \ll 1$. In this case $x_c \sim x_0 \ll 1$, and

the lower limit in the integral over $x$ may be set to zero; we then have, taking (13) into account,

$$J_\gamma \approx \int_{-c_0}^{c_0} \frac{dc}{(1-c)^2} \int_0^\infty \varphi(x)\,\frac{dx}{x} = \frac{20\pi}{3}\cdot\frac{c_0}{1-c_0^2}\ .$$

b) The case $x_0 \gg 1$. Changing the order of integration and repeating the manipulations from the preceding Appendix, we find that

$$J_\gamma \approx 4\sqrt{2}\int_{x_0}^{y_0}\frac{dx}{x^2}e^{-x}\int_{c_x}^{c_0}\frac{dc}{(1-c)^2} = \frac{8\sqrt{2}\,e^{-x_0}}{x_0^2(1-c_0)^2}\left[1+O\left(\frac{1}{x_0}\right)\right].$$

Appendix 4. Calculation of the integral $\varphi_{e\gamma}$ (32).

a) The case $\epsilon_0 \ll \omega_c$. We have $x \sim x_c \ll 1$, so that (the notation is the same as in (A4)):

$$J_{e\gamma} = \varphi_1\int_{-c_0}^{c_0}\frac{dc}{(1-c)(1+c)^2}\int_{x_c}^{\infty}\frac{dx}{x^{5/3}}\left(1-\frac{x_c}{x}\right)l = \frac{9\varphi_1}{10}\left(\frac{2}{3}\right)^{2/3} l\, f_2(\theta_0)\ ,$$

$$f_2(\theta_0) = \int_{-c_0}^{c_0}\frac{dc}{(1+c)^2(1-c)^{5/3}} = \frac{1}{2^{2/3}4}\left\{\frac{b}{a^3}-\frac{a}{b^3}+\frac{3}{2}\left(\frac{1}{a^2}-\frac{1}{b^2}\right)+\right.$$

$$\left.+\frac{5}{2}\left[\ln\frac{a(1-a)}{b(1-b)}+\frac{2}{\sqrt{3}}\operatorname{arctg}\frac{\sqrt{3}(b-a)}{2+b+a+2ab}\right]\right\} \qquad (A8)$$

Since the main contribution at small $\theta$ comes from the region $\theta \sim \pi - \theta_0$, $\omega_{2,1} \sim \epsilon_0\,(1 \pm c_0)$, we may set $\epsilon_f/\omega_1 \approx 1/(1 - c_0)$, whereupon

$$l = \ln\frac{E^2(1+c_0)}{m^2(1-c_0)}\ .$$

b) The case $x_0 \ll 1$, $y_0 \gg 1$. In this case, $\theta_0 \ll 1$ or $1 - c_0 \ll 1$. Just as in Appendix 2, upon changing the order of integration and discarding the integral over the region $x_0 > y_0$, we find that

$$J_{e\gamma} = \int_{x_0}^{y_0} \frac{dx}{x^2} \varphi(x) \int_{c_x}^{c_0} \frac{dc}{(1+c)^2(1-c)} \left(1 - \frac{x_c}{x}\right) l \quad . \tag{A9}$$

Since $1 - c_0 \ll 1$ and $c_0 - c_x \ll 1$, we may set $c = c_0$ in the expression for $l/(1 + c)^2$, after which the integral over $c$ may easily be performed. The main contribution to the integral over $x$ comes from the region $x \sim x_0$, where $\varphi(x) \approx \varphi_1 x^{1/3}$, so that

$$J_{e\gamma} = \frac{\varphi_1 l}{(1+c_0)^2} \int_{x_0}^{y_0} \frac{dx}{x^{5/3}} \left(\ln \frac{x}{x_0} - 1 + \frac{x_0}{x}\right) = \frac{27\varphi_1}{80} \frac{l}{x_0^{2/3}} . \tag{A10}$$

Since the main contribution comes from the region $\theta \sim \theta_0$, $\omega_1 \sim \epsilon_0$, $\omega_2 \sim \epsilon_0(1 - c_0)$, we may set $\epsilon_f/\omega_f \approx 1$ for the [processes] in (27), and we then have $l = \ln (E^2\theta_0^2/m^2)$.

c) The case $x_0 \gg 1$, $y_0 \gg 1$. In this case, expression (A9) (where $\varphi(x) = 4\sqrt{2}\, e^{-x}/x$) for $\varphi_{e\gamma}$ holds; we therefore have, after integration over $c$,

$$J_{e\gamma} = \frac{4\sqrt{2}\, l}{(1+c_0)^2} \int_{x_0}^{y_0} \frac{dx}{x^3} e^{-x} \left(\ln \frac{x}{x_0} - 1 + \frac{x_0}{x}\right).$$

The main contribution comes from the region $x - x_0 \sim 1$, where

$$\ln\frac{x}{x_0} - 1 + \frac{x_0}{x} \approx \frac{(x-x_0)^2}{2x_0^2},$$

Hence,

$$J_{e\gamma} = \frac{4\sqrt{2}}{x_0^5(1+c_0)^2} e^{-x_0} \ln\frac{E^2(1-c_0)}{m^2(1+c_0)} .$$

Appendix 5. Calculation of the integral $\Phi_{\gamma\gamma}$ (34).

a) The case $\epsilon_0 \ll \omega_e$. In this case, the main contribution comes from the region $x \sim x_c \ll 1$, $y \sim y_c \ll 1$, where we may use the asymptotic expression $\varphi(x)$ for $x \ll 1$ (12):

$$J_{\gamma\gamma} = P_1^2 \int_{-c_0}^{c_0} \frac{dc}{1-c^2} \int_{x_c}^{\infty} \frac{dx}{x^{5/3}} \int_{xy_c/(x-x_c)}^{\infty} \frac{dy}{y^{5/3}} = \left(\frac{2\omega_c}{\epsilon_0}\right)^{4/3} \frac{3P_1^2\Gamma(2/3)\Gamma(5/3)}{2\Gamma(7/3)} f_3(\theta_0),$$

$$f_3(\theta_0) = \int_{-c_0}^{c_0} \frac{dc}{(1-c^2)^{5/3}} .$$

b) The case $x_0, y_0 \gg 1$. In this case, $x_c \gg 1$, $y_c \gg 1$, so that, using the asymptotic expressions for $\varphi(x)$ and $\varphi(y)$ at large $x$ and $y$ (12), we obtain the following after integrating over $y$ and making the substitution $x = x_c t$:

$$J_{\gamma\gamma} = \frac{2^{11}}{Z^5} \int_0^{c_0} \frac{dc}{(1-c)^3(1+c)^4} I(c); \quad I(c) = \int_1^{\infty} f(t) e^{-x_c\varphi(t)} dt;$$

$$f(t) = \frac{(t-1)^3}{t^6}, \quad \varphi(t) = t + \lambda^2 \frac{t}{t-1}, \quad \lambda = \sqrt{\frac{y_c}{x_c}} = \operatorname{ctg}\frac{\theta_0}{2} . \qquad (A11)$$

Since $x_c \gg 1$, it is convenient to use the method of steepest descent to calculate $I(c)$:

$$I(c) = \left(\frac{2\pi}{x_c \varphi''(t_0)}\right)^{1/2} f(t_0)\, e^{-x_c \varphi(t_0)},$$

where $t_0$ is the minimum point for the function $\varphi(t)$, and $\varphi(t_0) = (1 + \lambda)^2$, $\varphi''(t_0) = 2(1 + \lambda)^4/\lambda$, and $f(t_0) = \lambda^3/(1 + \lambda)^4$. Upon substituting these expressions into (A11), we obtain (substitution $z \sin\theta = u$)

$$J_{\gamma\gamma} = \frac{2^8\sqrt{2\pi}}{z^3 c_0 (1+s_0)^3} e^{-z} \int_{2s_0}^{\infty} \frac{du}{u^{7/2}} e^{-u} \simeq \frac{2^8\sqrt{2\pi}}{z^3 c_0 (1+s_0)^3 (2s_0)^{7/2}} e^{-2(1+s_0)}.$$

c) The case $y_0 \gg 1$, $x_0 y_0 \ll 1$. In this case, we must have $\theta_0 \ll 1$. In view of the symmetry of $\mathcal{F}_{\gamma\gamma}$ with respect to the change of variables $c \to -c$, we have

$$J_{\gamma\gamma} = 2 \int_0^{c_0} \frac{dc}{1-c^2} \int_{x_c}^{\infty} \frac{dx}{x^2} \varphi(x) \int_{xy_c/(x-x_c)}^{\infty} \frac{4\sqrt{2}}{y^3} e^{-y} dy,$$

where we have used the asymptotic expression for $\varphi(y)$ at large $y$, since $y_c \gg 1$ for $c \geq 0$. After integration over $y$, it is convenient to change the order of integration. Disregarding the contribution from the region $x > y_0$, we find that

$$J_{\gamma\gamma} = \frac{2^6\sqrt{2}}{z^3} \int_{x_0}^{y_0} \frac{dx}{x^2} \varphi(x) \int_{c_x}^{c_0} \frac{dc}{(1-c)(1+c)^4} \left(1 - \frac{x_c}{x}\right)^3 e^{-xy/(x-x_c)}.$$

The integration over c may conveniently be carried out if we make the substitution $t = xy_c/(x - x_c)$, after which

$$J_{\gamma\gamma} = \frac{8\sqrt{2}}{z^5(1-c_0)} e^{-z} I, \quad I = \int_{x_0}^{y_0} \frac{dx}{x} \varphi(x) e^{-x_0 y_0/(x-x_0)}.$$

To evaluate the remaining integral, I, we break the region of integration up into two intervals $x_0 \le x \le \sqrt{x_0 y_0}$ and $\sqrt{x_0 y_0} \le x \le y_0$. The contribution from the first interval is small, since

$$I_1 < \int_{x_0}^{\sqrt{x_0 y_0}} \frac{dx}{x} \varphi(x) \approx 3\varphi_1 (x_0 y_0)^{1/3} \ll 1.$$

On the second interval, the exponent $x_0 y_0/(x - x_0) < \sqrt{x_0 y_0} \ll 1$, so that

$$I \approx \int_{\sqrt{x_0 y_0}}^{y_0} \frac{dx}{x} \varphi(x) \approx \int_0^{\infty} \frac{dx}{x} \varphi(x) = \frac{10\pi}{3}.$$

Appendix 6.

We shall now present some approximate formulae for small angles $\theta_0$ $(m/E \ll \theta_0 \ll 1)$, where the quantities E, $\omega_c$, and $\epsilon_0$ are given in GeV, $z = \epsilon_0/\omega_c$, and $x_0 = \epsilon_0 \theta_0^2/4\omega_c$.

1. The process $\gamma\gamma \to e^+e^-$:

$$N_{\gamma\gamma \to e^-} = \begin{cases} \dfrac{1{,}3\, e^{-z}}{(\epsilon_0\theta_0)^{4/3} (E/100)^2}, & z \lesssim 1 \\ \dfrac{2{,}7\, e^{-z}}{(\epsilon_0\theta_0)^2 z^3 (E/100)}, & z \gg 1 \end{cases}$$

Analogous formulae exist for the process $\gamma\gamma \to \mu^+\mu^-$ when $\epsilon_0 \gg m_\mu$.

2. Compton scattering $\gamma e^- \to \gamma e^-$:

$$N_{\gamma e^- \to e^-} = \frac{1{,}1 \cdot 10^{-2}}{(\varepsilon_0 \theta_0^2)^{2/3} (E/100)^2} e^{-X_0}, \qquad X_0 \lesssim 1;$$

$$N_{\gamma e^- \to \gamma} = \frac{3{,}6 \cdot 10^{-4}}{(E\theta_0/100)^2} e^{-X_0}, \qquad X_0 \lesssim 1.$$

3. The process $\gamma e^- \to e^- e^+ e^-$:

$$N_{\gamma e^- \to e^-} = \frac{1{,}5 \cdot 10^{-3}}{\varepsilon_0^{5/3} (E/100)} e^{-X_0} \begin{cases} \frac{1}{\theta_0^2} \ln \frac{E^2}{m^2 \theta_0^2}, & Z \lesssim 1 \\ \frac{1}{\theta_0^{4/3}} \ln \frac{(E\theta_0)^2}{m^2}, & Z \gg 1, \; X_0 \lesssim 1. \end{cases}$$

4. Brehmsstrahlung $e^+e^- \to e^+e^-\gamma$:

$$N_{e^+e^- \to e^-} = \frac{3 \cdot 10^{-5}}{\varepsilon_0 \theta_0^2 (E/100)} \ln \frac{E^2}{(m\theta_0)^2};$$

$$N_{e^+e^- \to \gamma} = \frac{2{,}5 \cdot 10^{-6}}{(E\theta_0/100)^2} \ln \frac{E}{\varepsilon_0} \ln \frac{E^2}{m^2}.$$

5. The process $e^+e^- \to e^+e^-e^+e^-$:

$$N_{e^+e^- \to e^-} = \frac{7 \cdot 10^{-6}}{(\varepsilon_0 \theta_0)^2} \left( \ln \frac{E^2}{m^2} \right)^2.$$

The number of background events for the processes $\gamma\gamma \to e^+e^-\gamma$ and $\gamma e \to ee^+e^-\gamma$ in which a photon is recorded differs from the number of background events without

emission of a photon by an additional factor $\sim(\alpha/\pi)$ ln $(\epsilon_0^2\theta_0^2/m^2)$.

REFERENCES

[1] V. E. Balakin, G. I. Budker, A. N. Skrinsky. Preprint INP 78-101, Novosibirsk, 1978.
V. E. Balakin. Report of the Working Conference on the Experimental Program for $e^+e^-$ Beam Colliders (19-23 November 1979), Novosibirsk, 1979, p. 60 [in Russian]

[2] V. E. Balakin, G. I. Budker, and A. N. Skrinskii. Proceedings of the 6th All-Union Accelerator Conference. Dubna, 1978 [in Russian].

[3] L. D. Landau and E. M. Lifshitz Field Theory, Nauka, 1973.

[4] V. N. Baier, E. A. Kuraev, V. S. Fadin, and V. A. Khoze. Materials for the XV Winter School of the Leningrad Institute for Nuclear Physics, Leningrad, 1980, p. 84 [in Russian].
Physics Reports, in press.

[5] V. S. Fadin and V. A. Khoze. Pis'ma v Zh. Eksp. Teor. Fiz., 17, 438, 1973.

Received 22 June 1981